Localization of a portion of the liver isoform of fatty-acid-binding protein (L-FABP) to peroxisomes

Vasily D. ANTONENKOV*[1], Raija T. SORMUNEN†, Steffen OHLMEIER*, Leen AMERY‡, Marc FRANSEN‡, Guy P. MANNAERTS‡ and J. Kalervo HILTUNEN*[1]

*Department of Biochemistry, Biocenter Oulu, University of Oulu, Linnanmaa, P.O. Box 3000, FIN-90014 Oulu, Finland, †Department of Pathology, Biocenter Oulu, University of Oulu, Linnanmaa, P.O. Box 3000, FIN-90014 Oulu, Finland, and ‡Departement Moleculaire Celbiologie, Katholieke Universiteit Leuven, Campus Gasthuisberg, Afdeling Farmakologie, Herestraat 49 (box 601), B-3000 Leuven, Belgium

The liver isoform of fatty-acid-binding protein (L-FABP) facilitates the cellular uptake, transport and metabolism of fatty acids and is also involved in the regulation of gene expressions and cell differentiation. Consistent with these functions, L-FABP is predominantly present in the cytoplasm and to a lesser extent in the nucleus; however, a significant portion of this protein has also been detected in fractions containing different organelles. More recent observations, notably on L-FABP-deficient mice, indicated a possible direct involvement of L-FABP in the peroxisomal oxidation of long-chain fatty acids. In order to clarify the links between L-FABP and peroxisomal lipid metabolism, we reinvestigated the subcellular distribution of the protein. Analytical subcellular fractionation by a method preserving the intactness of isolated peroxisomes, two-dimensional gel electrophoresis of peroxisomal matrix proteins combined with MS analysis, and immunoelectron microscopy of liver sections demonstrate the presence of L-FABP in the matrix of peroxisomes as a soluble protein. Peroxisomal L-FABP was highly inducible by clofibrate. The induction of L-FABP was accompanied by a marked increase in the binding capacity of peroxisomal matrix proteins for oleic acid and *cis*-parinaric acid. The peroxisomal β-oxidation of palmitoyl-CoA and acyl-CoA thioesterase activity were stimulated by L-FABP, indicating that the protein modulates the function of peroxisomal lipid-metabolizing enzymes. The possible role of intraperoxisomal L-FABP in lipid metabolism is discussed.

Key words: clofibrate, fatty-acid-binding protein, liver, β-oxidation, rat peroxisome, sterol carrier protein 2 (SCP-2).

INTRODUCTION

The intracellular FABPs (fatty-acid-binding proteins) belong to a superfamily of lipid-binding proteins and are abundantly expressed in vertebrate tissues. These low molecular mass proteins (14–15 kDa) exhibit distinct expression patterns specific for each tissue and are classified according to their predominant location, e.g. L-FABP, the liver isoform of FABP. L-FABP (other names: Z protein, haem-binding protein and hepatic FABP) is highly expressed in the liver where it represents 2–5 % of the total cytosolic protein. It is also expressed, although to a lesser extent, in small intestine, colon and kidney. L-FABP interacts with a wide range of ligands, including long-chain and very-long-chain fatty acids (saturated, unsaturated and branched-chain fatty acids), fatty acyl-CoAs, haem, lysophosphatidic acid, eicosanoids and hypolipidaemic drugs such as fibrates known as peroxisome proliferators (reviewed in [1,2]). Results of binding assays confirmed by crystallographic analysis indicate that contrary to other members of the FABP family that interact with NEFA (non-esterified fatty acids) and fatty acyl-CoAs in a 1:1 stoichiometry, each molecule of L-FABP possesses two binding sites for these ligands [2].

The level of L-FABP expression in rodent liver is regulated in concert with peroxisome proliferation. This pleiotropic cellular response to a range of natural (unsaturated long-chain fatty acids and phytanic acid) and chemically synthesized (some hypolipidaemic drugs) compounds is characterized mainly by a profound increase in the activity of peroxisomal and mitochondrial β-oxidation enzymes (reviewed in [3]). The peroxisome proliferators influence lipid metabolism through activation of PPARα (peroxisome-proliferator-activated receptor α), which in turn regulates the transcription of a wide variety of proteins, including the β-oxidation enzymes [3]. It has been shown that both natural and chemically synthesized peroxisome proliferators increase the gene expression and the synthesis of L-FABP [4,5]. Previous results indicate that L-FABP may participate in the transport of PPARα ligands into the nucleus and regulate transcription of the PPARα-responsive genes via a direct protein–protein interaction with the receptor [6].

Several studies, conducted mainly in the 1980s, were dedicated to the subcellular distribution of L-FABP. More than 90 % of the protein was found in the cytoplasm [7–10]. A substantial portion of it was also detected in the nucleus [11,12]. Some results indicated an interaction of L-FABP with the cytoplasmic side of the endoplasmic reticulum and mitochondrial outer membranes [7,11]. This interaction might be functionally relevant in view of the stimulation by L-FABP of microsomal acyl-CoA:cholesterol acyltransferase activity *in vitro* [13] and in transfected cells [14] and the modulation of microsomal phospholipid synthesis [15]. Attempts to reveal a peroxisomal localization of L-FABP were without success [8,12,16]. These results led to the conclusion that L-FABP is responsible for binding of lipophilic ligands in the cytoplasm, whereas in peroxisomes this function would be carried out by SCP-2 (sterol carrier protein 2) (reviewed in [17]).

Experiments with cell lines including cells stably expressing L-FABP confirmed the role of the protein in cellular uptake of fatty acids and their utilization through rapid incorporation into

Abbreviations used: CHO cells, Chinese-hamster ovary cells; DTT, dithiothreitol; FABP, fatty-acid-binding protein; GFP, green fluorescent protein; LACS4, long-chain acyl-CoA synthetase 4; L-FABP, liver isoform of FABP; NEFA, non-esterified fatty acid; PEG 1500, poly(ethylene glycol) 1500; PMP22, peroxisomal membrane protein with a monomeric molecular mass of 22 kDa; PPARα, peroxisome-proliferator-activated receptor α; PTS, peroxisomal targeting signal; SCP-2, sterol carrier protein 2.

[1] Correspondence may be addressed to either of these authors (email vasily.antonenkov@oulu.fi or kalervo.hiltunen@oulu.fi).

triacylglycerols and phospholipids [18]. A marked reduction in fatty acid uptake from the plasma and a decrease in intracellular triacylglycerol level were detected in L-FABP-deficient mice [19,20]. Further study using isolated hepatocytes from L-FABP knockout mice led to the conclusion that the intracellular level of L-FABP may directly affect the rate of fatty acid β-oxidation in mitochondria and/or peroxisomes, especially during fasting [21]. L-FABP gene ablation also decreased branched-chain fatty acid metabolism [22]. Experiments with cultured primary hepatocytes isolated from livers of L-FABP$^{-/-}$ mice revealed an inhibition of the peroxisomal oxidation and microsomal esterification of phytanic acid [23]. In contrast, L-FABP expression in cultured cells enhanced phytanic acid metabolism mainly by increasing the rate of its peroxisomal oxidation [24]. These recent observations imply that L-FABP might be directly involved in the oxidation of long straight- and branched-chain fatty acids in peroxisomes.

The potential role of L-FABP in peroxisomal lipid metabolism prompted us to reinvestigate the subcellular distribution of the protein paying special attention to its possible localization in peroxisomes. In the present study, we show that a portion of L-FABP is a *bona fide* peroxisomal protein. The quantity of L-FABP in peroxisomes is significantly increased after treatment of rats with the peroxisome proliferator clofibrate.

MATERIALS AND METHODS

Materials

Percoll (colloidal suspension of silica) and ion exchangers were purchased from Amersham Biosciences. The other chemicals were from Sigma except those for which sources are indicated.

Animals and subcellular fractionation

The use of experimental animals was approved by the committee on animal experimentation at the University of Oulu. Male Sprague–Dawley rats weighing 200–250 g were used. Clofibrate-treated rats were maintained for 2 weeks on a standard diet containing 0.3 % (v/w) clofibrate. For subcellular fractionation, the livers were homogenized in isolation medium-1 [0.25 M sucrose, 10 mM Mops, pH 7.4, 1 mM EDTA, 1 mM EGTA, 2 mM DTT (dithiothreitol), 0.1 % (v/v) ethanol and 0.1 mM PMSF] or in isolation medium-2 [0.16 M sucrose, 12 % (w/v) poly(ethylene glycol) 1500 (PEG 1500), 10 mM Mops, pH 7.4, 1 mM EDTA, 1 mM EGTA, 2 mM DTT, 0.1 % ethanol and 0.1 mM PMSF]. The isolation of highly purified peroxisomes was carried out exactly as described in [25]. In some experiments, the homogenates were centrifuged at 1500 ***g*** for 12 min and the resulting post-nuclear supernatant was loaded on multistep Nycodenz [32 ml of 16–50 % (w/v) Nycodenz] or Optiprep [32 ml of 20–50 % (w/v) Optiprep] gradients prepared with isolation medium-1 containing no sucrose. The samples were centrifuged in a vertical VTi 50 rotor (Beckman) at 100 000 ***g*** for 90 min in slow acceleration and deceleration mode.

Treatment of purified peroxisomes

Disruption of peroxisomes by sonication and separation of the main peroxisomal constituents (membrane, nucleoid and matrix proteins) by sucrose-density-gradient centrifugation was conducted as described in [25]. For proteinase treatment and immunoprecipitation experiments, purified peroxisomes were slowly diluted (10 times) by the dropwise addition of 20 mM Mops (pH 7.4) to prevent osmotic damage of the particles (see [25] for more details). Peroxisomes were then sedimented at 36 000 ***g*** for 45 min and resuspended in 20 mM Mops (pH 7.4) containing 4 % Optiprep. For proteinase treatment, aliquots of peroxisomes (0.4 mg of protein/ml) were incubated with proteinase K (0.6 unit/ml) at 37 °C. The reaction was stopped by 1 mM PMSF. For immunoprecipitation of L-FABP, aliquots (500 μl) of peroxisomes (0.6 mg of protein/ml) were incubated for 40 min at 4 °C with Triton X-100 (0.05 %, w/v) and affinity-purified anti-FABP antibodies coupled with Affi-Gel Hz beads as described by the manufacturer (Bio-Rad). The beads were then sedimented and the supernatants were used for SDS/PAGE and immunoblotting.

Assay of enzymes

The protein content and the marker enzymes (glutamate dehydrogenase, mitochondria; esterase, endoplasmic reticulum; acid phosphatase, lysosomes; L-α-hydroxyacid oxidase, peroxisomes; and phosphoglucose isomerase, cytosol) were determined as described in [26,27]. Activity measurements of catalase (matrix proteins), urate oxidase (nucleoid) and NADH:cytochrome *c* reductase (membrane) were used to detect the subperoxisomal localization of peroxisomal constituents [27]. Peroxisomal palmitoyl-CoA β-oxidation was followed by measuring the reduction of NAD^+ at 340 nm. The standard incubation medium (22 °C) contained 20 mM Tris/HCl (pH 8.0), 0.2 mM NAD^+, 0.1 mM CoA, 1.0 mM sodium azide, 1 mM DTT, 50 μM palmitoyl-CoA, 0.06 % (w/v) BSA and 30–40 μg of peroxisomal protein. The effect of L-FABP on the enzymatic activities (see the Results section) was studied using a fraction containing only soluble matrix proteins to avoid partition of acyl-CoA esters into the peroxisomal membrane. Purified peroxisomes were disrupted by sonication (6 cycles, 15 s each, amplitude 15 μm; Soniprep 150; Sanyo) in 50 mM Tris/HCl (pH 8.2). The released matrix proteins were separated from membrane fragments by centrifugation at 100 000 ***g*** for 60 min. The recovery of the β-oxidation activity was 50–60 % relative to whole peroxisomes. Acyl-CoA thioesterase activity (standard assay) was measured at 412 nm using a medium (22 °C) containing 20 mM Hepes (pH 7.8), 20 μM acyl-CoA tested, 0.02 % BSA and 0.05 mM DTNB [5,5′-dithiobis-(2-nitrobenzoic acid)]. A molar absorption coefficient (ε_{412}) of 13 600 $M^{-1} \cdot cm^{-1}$ was used to calculate the activity. Units of enzyme activity are expressed as nmol of substrate consumed or product formed per min.

Purification of L-FABP

Native L-FABP was isolated from homogenates of clofibrate-treated rat livers as described in [28] with some modifications. Briefly, the homogenates were prepared in isolation medium-1 and centrifuged at 100 000 ***g*** for 60 min. The resulting supernatant was treated with ammonium sulphate (70 % saturation) and the proteins were sedimented at 25 000 ***g*** for 1 h. The L-FABP-containing supernatant was desalted and subjected to QAE (quaternary aminoethyl)-anion exchange followed by size-exclusion (Sephadex G-50) chromatography. The fractions enriched in L-FABP were combined and passed subsequently over Econo-Pac High S cartridge (Bio-Rad), phosphocellulose and Sephadex G-50 columns. Detection of L-FABP in the column fractions was carried out by immunoblotting with the anti-L-FABP antibodies (a gift from Professor J. H. Veerkamp, University Medical Center Nijmegen, Nijmegen, The Netherlands). The purity of the isolated L-FABP was verified by SDS/PAGE and fluorescence emission spectroscopy [28]. The purified L-FABP fraction contained no admixture of SCP-2, as was confirmed by using anti-SCP-2 antibodies.

Two-dimensional gel electrophoresis and protein identification

The peroxisomal matrix proteins were precipitated with 80 % (v/v) acetone and resuspended in urea buffer [8 M urea, 2 M thiourea, 1 % (w/v) CHAPS, 20 mM DTT, 0.8 % (v/v) carrier ampholytes 3–10, 100 mM Tris/HCl, pH 7.5, 1 mM EDTA and 14 μM PMSF]. The two-dimensional gel electrophoresis was performed as described in [29]. The gels were stained with the SYPRO Ruby dye (Bio-Rad), which allows for the semi-quantitative estimation of the protein content. Excised spots were in-gel-digested and identified from the peptide 'fingerprints' [29]. The identification of a protein was accepted if the peptides (mass tolerance 20 p.p.m.) covered at least 30 % of the complete sequence.

Transfection studies and binding of recombinant L-FABP to Pex5p *in vitro*

For the *in vivo* analysis of the targeting of L-FABP, plasmids coding for full-length L-FABP (pLA65) and L-FABP without the C-terminus (KRI) (pLA67) with a GFP (green fluorescent protein) tag at the N-terminus were constructed. For construction of the pLA65 plasmid, human liver cDNA was used to amplify the full-length L-FABP cDNA by PCR with the forward (5′-GAGGG**AGATCT**ATTGCCACCATGAGTTTC) and reverse (5′-GAAATG**GGTACC**TGTTTAAATTCTCTTGC) primers containing the BglII and KpnI restriction sites respectively (shown in boldface). The PCR product was gel-purified, digested with KpnI/BglII, and subcloned into the KpnI/BglII-digested pEGFP-C1 vector (ClonTech). The pLA67 construct was made in a similar manner. The cDNA was amplified using the same forward primer as for the full-length protein and the reverse primer 5′-GAAATG**GGTACC**TGTTTGAATTCTCTAGC containing a KpnI restriction site. CHO cells (Chinese-hamster ovary cells) were transiently transfected by the polyethylenimine transfection method and processed for (in)direct fluorescence microscopy [30]. In some experiments, cytosol was washed out by permeabilization of the CHO cells to reveal an apparent presence of L-FABP–GFP fusion protein in subcellular organelles. To perform interaction studies with the PTS1 (peroxisomal targeting signal 1) receptor Pex5p, the N-terminally His-tagged L-FABP fusion construct was prepared by subcloning the BglII/KpnI-restricted full-length L-FABP cDNA generated by PCR into the KpnI/BglII-digested pBadHisB vector (ClonTech). The construct was expressed in *Escherichia coli* and the recombinant fusion protein was isolated by using Ni^{2+}-nitrilotriacetate–agarose. Blot overlay assays were performed as described in [31].

Electron microscopy

For immunoelectron microscopy, fresh liver samples were fixed for 2 h in 4 % (w/v) paraformaldehyde in 0.1 M sodium phosphate (pH 7.4) containing 2.5 % (w/v) sucrose. For immunolabelling, the thin sections were incubated in PBS containing 0.05 M glycine for 15 min followed by incubation with 5 % BSA in PBS containing 0.1 % (w/v) cold water fish skin gelatin (Aurion) for 30 min. The sections were then incubated with primary antibodies (diluted 1:400) for 60 min followed by incubation with a Protein A–gold complex (10 nm gold particles) for 30 min [32]. The control samples were prepared by carrying out the labelling procedure without antibodies.

Delipidation of proteins

A portion of the proteins was mixed with an equal volume of 20 % (w/v) Lipidex™-1000 (PerkinElmer) prepared on 10 mM Mops (pH 7.2). After 1 h incubation at 37 °C with gentle shaking, Lipidex™-1000 was removed by centrifugation at 4000 ***g*** for 10 min and the resulting supernatant was filtered through a membrane (0.22 μm; Millipore). All protein of the sample was recovered in the filtrate.

Size-exclusion chromatography of peroxisomal matrix proteins and detection of the fatty acid binding capacity

Detection of the fatty acid binding capacity was done as described in [20] with some modifications. A Superdex™75 HR column connected to a SMART™ system (Amersham Biosciences) was equilibrated with PBS (pH 7.4) and calibrated with protein standards (Sigma). Delipidated peroxisomal matrix proteins (1.0 mg), concentrated by using a membrane device with a 5 kDa cut-off, were incubated with 20 nmol of [^{3}H]oleic acid (specific radioactivity 8.0 Ci/mmol; Amersham Biosciences) for 5 min at 4 °C and loaded on to the column. The elution was done at 4 °C with PBS (pH 7.4) at a flow rate of 400 μl/min and 0.5 ml fractions were collected. Aliquots (100 μl) were used to measure ^{3}H content by liquid-scintillation counting (WinSpectral™; Wallac). Fractions were also analysed by Western blotting for the presence of L-FABP and SCP-2. Determination of the capacity of peroxisomal matrix proteins to bind *cis*-parinaric acid was performed exactly as described in [33].

Other methods

A rabbit antiserum against rat L-FABP was generated according to standard methods (see [34]). The sources of other antibodies have been described in [25,34]. The antibodies used for immunoelectron microscopy were partially purified by ammonium sulphate precipitation and size-exclusion chromatography. SDS/PAGE using 15 % (w/v) Criterion Precast gels (Bio-Rad) or 10 % (w/v) polyacrylamide gels, Coomassie Blue staining, silver staining and immunoblotting were carried out as described in [34]. To quantify L-FABP, the Rat L-FABP ELISA test kit (HyCult Biotechnology) has been used.

RESULTS

Effect of PEG 1500 on the subcellular distribution of L-FABP

During isolation, mammalian peroxisomes suffer an osmotic lysis that is resistant to commonly used osmoprotectors such as sucrose [25,35]. In order to avoid osmotic damage to peroxisomes, we reinvestigated the subcellular distribution of L-FABP by using PEG 1500 as an osmoprotector. As we found recently [25], this compound is highly effective to preserve the intactness of peroxisomes during isolation. As expected, PEG 1500 partially prevented leakage of the soluble matrix protein thiolase from peroxisomes during differential (Figure 1A) and isopycnic (Figure 1B) centrifugation of a rat liver homogenate, while it had no effect on the subcellular distribution of the peroxisomal membrane marker PMP22 (peroxisomal membrane protein with monomeric molecular mass of 22 kDa) and the cytosolic enzyme glutathione S-transferase (results not shown). Importantly, PEG 1500 visibly affected the subcellular distribution of L-FABP. The quantity of the protein in fractions enriched in peroxisomes, the L-fraction obtained after differential centrifugation (Figure 1A) and the bottom fractions of the Nycodenz gradient (Figure 1B) was substantially higher in samples containing PEG 1500 relative to control without this osmoprotector. The results indicate that rat liver peroxisomes might harbour L-FABP as a soluble matrix protein.

Co-purification of a portion of L-FABP with normal liver peroxisomes

To isolate peroxisomes, we used a newly developed method [25], which consists of two steps: (i) the centrifugation of a post-nuclear

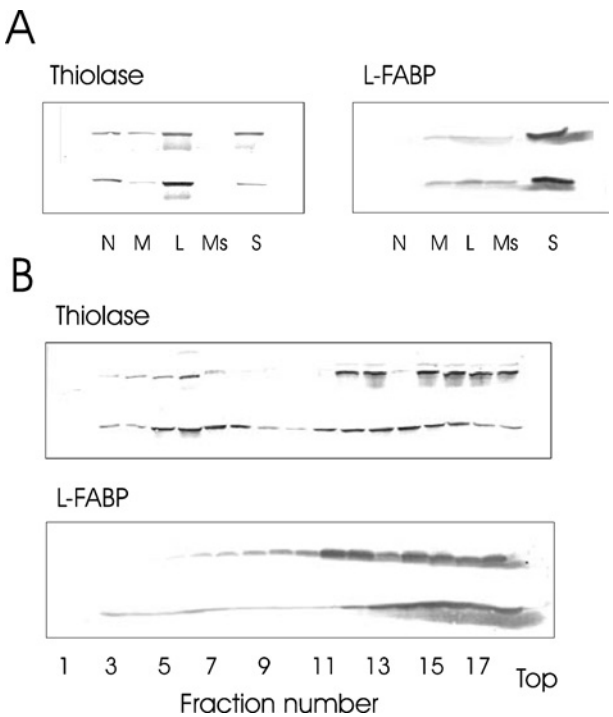

Figure 1 Effect of PEG 1500 on the subcellular distribution of L-FABP

Rat liver homogenates were prepared using isolation medium-1 (see the Materials and methods section), which contains 0.25 M sucrose (**A**, **B**, upper bands), or with isolation medium-2 containing 12 % PEG 1500 (**A**, **B**, lower bands). (**A**) The homogenates were fractionated by differential centrifugation into a nuclear (N), a heavy mitochondrial (M), a light mitochondrial (L), a microsomal (Ms) and a cytosolic (S) fraction. According to the marker enzyme activity analysis, the light mitochondrial fraction is enriched with peroxisomes. Immunoblot analysis was performed with equal amounts of protein. (**B**) Nycodenz density gradient centrifugation of the post-nuclear supernatant. Note that according to the marker enzyme activities (results not shown), gradient fractions 3–8 were enriched in peroxisomes, while fractions 14–18 contained cytosol. Immunoblots were performed with an equal volume of each fraction.

liver homogenate in a self-generated Percoll gradient (Figure 2A) followed by (ii) Optiprep density gradient centrifugation (Figure 2B). The localization of peroxisomes in gradient fractions was established by immunodetection of thiolase (Figures 2A and 2B). The distribution of L-FABP over the Percoll gradient shows that, as expected, L-FABP was abundantly present in the fractions containing cytoplasmic proteins (see Figure 2A, fractions 18–24). A small portion of L-FABP was also detected in the bottom fractions of the gradient (fractions 1–3), which together with intact peroxisomes also contain some mitochondria and lysosomes. Further purification of the peroxisome-enriched fractions by means of Optiprep gradient centrifugation (see Figure 2B) revealed co-migration of a small portion of L-FABP with the peroxisomal proteins thiolase and SCP-2. The composition of the purified peroxisomal fraction was deduced from the specific activities of marker enzymes for the different subcellular compartments [26]. According to this estimation, peroxisomes contributed more than 95 % to the total protein content of the fraction. These results were confirmed by electron microscopic examination showing a nearly homogeneous population of peroxisomes (results not shown). SDS/PAGE of the purified peroxisomes revealed a significant amount of polypeptides with a molecular mass of 12–14 kDa (marked by an asterisk in Figure 2C). Immunodetection of L-FABP in the same peroxisomal preparation led to the appearance of only one band. Immunostaining with antibodies generated against the known peroxisomal matrix protein SCP-2 showed two bands: one of 12–14 kDa and a second one of 60 kDa, which reflect the positions in the gel of SCP-2 and SCP-2/3-oxoacyl-CoA thiolase respectively [34].

In order to determine whether or not L-FABP was located inside peroxisomes, the purified particles were treated with proteinase K or with immobilized anti-L-FABP antibodies in the absence or presence of 0.05 % Triton X-100 (Figures 2D and 2E). In the absence of detergent, the proteinase did not significantly degrade the peroxisomal matrix proteins catalase (results not shown) and thiolase (Figure 2D). Incubation of the detergent-treated peroxisomes with proteinase K led to disappearance of the immunosignals corresponding to these proteins. Under the same conditions, L-FABP behaved similarly to the peroxisomal matrix proteins tested, suggesting that it is located inside the particles. This was confirmed by incubation of purified peroxisomes with immobilized anti-L-FABP antibodies. The antibodies specifically affect the content of L-FABP in the peroxisomal preparations treated with Triton X-100 (Figure 2E). Sonication of the purified peroxisome fraction and separation of the peroxisomal 'ghosts' from the released proteins by sucrose-density-gradient centrifugation revealed that even moderate damage to the membrane caused by mild sonication led to extensive leakage from peroxisomes of L-FABP together with other soluble matrix proteins, e.g. thiolase (results not shown).

Effect of clofibrate on the content of L-FABP in peroxisomes

Isopycnic centrifugation of a liver post-nuclear homogenate from clofibrate-treated animals in an Optiprep density gradient led to the effective separation of peroxisomes from other cellular constituents as illustrated by the gradient distribution of marker enzyme activities (Figure 3A). Therefore this approach enabled us to analyse directly the distribution of proteins between peroxisomes and cytosol. The relatively high purity of peroxisomes isolated by Optiprep gradient centrifugation (85–88 % of the total protein content in the fraction; results not shown) was sufficient for the estimation of the effect of clofibrate on the content of L-FABP and other proteins in the particles (see below). In agreement with previous reports (see [3]), the content in the peroxisomal fraction of proteins such as PMP70 (results not shown) and thiolase (Figures 3B and 3C) had increased severalfold. However, in the same fraction, clofibrate only slightly increased the total quantities of catalase and SCP-2 (Figure 3B), while the relative content of these proteins in the particles (Figure 3C) was the same (catalase) or even decreased (SCP-2), most probably owing to the concomitant induction of other peroxisomal proteins, especially the β-oxidation enzymes. Noteworthily, the total amount of L-FABP in peroxisomes (Figure 3B) and its concentration in these organelles (Figure 3C) were increased significantly. An ELISA test (Figure 3D) showed that in normal rat liver the relative content of L-FABP in peroxisomes is low. Treatment with clofibrate leads to an increase in the concentrations of L-FABP in peroxisomes and cytosol, although the induction in peroxisomes was much higher.

Two-dimensional electrophoresis of soluble peroxisomal proteins and identification of peroxisomal L-FABP by MS

The low intensity of the immunosignal obtained in peroxisomal preparations with the polyclonal antibodies which we used to detect L-FABP might cast some doubt on the specificity of the observed signal. In order to address this issue, we used two-dimensional gel electrophoresis in combination with MS as an independent approach to verify the presence of L-FABP in peroxisomes. The two-dimensional gel electrophoresis of peroxisomal matrix proteins extracted by sonication resulted in more than 400 spots detectable in a SYPRO Ruby dye-stained gel (Figure 4A). The protein pattern obtained for normal liver peroxisomes (results

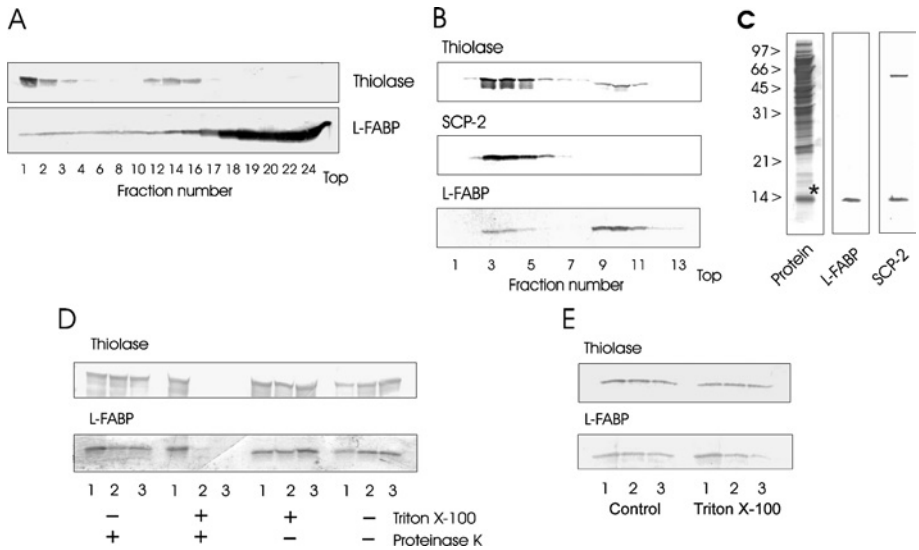

Figure 2 Localization of a portion of L-FABP in normal rat liver peroxisomes

(**A**) Percoll gradient centrifugation of a post-nuclear supernatant. (**B**) Optiprep density gradient centrifugation of the fractions obtained from a Percoll gradient. Immunoblots (**A**, **B**) were prepared with equal volumes of the fractions. (**C**) Protein pattern of purified peroxisomes and immunodetection of L-FABP and SCP-2. Total peroxisomal proteins were subjected to SDS/PAGE and silver-stained (left panel) or blotted and incubated with antibodies raised against L-FABP (middle panel) or SCP-2 (right panel). The molecular mass (kDa) of the marker proteins is indicated on the left. The asterisk in the left panel indicates a 12–14 kDa protein band. (**D**) Proteinase treatment of peroxisomes. Peroxisomes purified from clofibrate-treated rat livers were incubated at 37 °C in the presence of proteinase K (0.6 unit/ml) and/or Triton X-100 (0.05 %) for 0 min (condition 1), 30 min (condition 2) or 70 min (condition 3). (**E**) Immunoprecipitation of L-FABP. Peroxisomes were incubated with the immobilized anti-FABP antibodies in the absence (Control) or presence (Triton X-100) of detergent. Immunoblots of peroxisomal proteins remaining in the supernatant after immunoprecipitation are shown. Condition 1, no beads; 10 μl (condition 2) or 30 μl (condition 3) of swelled IgG beads was added to 500 μl of peroxisomes. Control incubations with the same amounts of beads that were not coupled with antibodies did not affect the content of L-FABP in the peroxisomal preparations (results not shown).

not shown) was clearly different from that of clofibrate-treated animals (see Figure 4A), including the gel region of 12–14 kDa proteins. The main protein spots in this region were excised and in-gel-digested. By means of the peptide 'fingerprints' measured by MALDI–TOF (matrix-assisted laser-desorption ionization–time-of-flight) MS, two proteins corresponding to the spots marked on the gel (Figure 4A) were unambiguously identified as L-FABP (Figure 4B) and SCP-2 (results not shown). Comparison of the protein quantities in the gel revealed a much higher content of L-FABP relative to SCP-2 in proliferated peroxisomes (Figure 4C). In contrast, the content of L-FABP in normal peroxisomes was substantially lower compared with SCP-2 (results not shown).

Immunoelectron microscopy of liver cells with antibodies against L-FABP

Immunogold labelling of liver samples from normal rats revealed a predominantly cytosolic localization of L-FABP. Nuclei were also stained. The labelling of peroxisomes was hardly detectable (Figure 5A). As a control, we performed immunolabelling on the same sections with antibodies against peroxisomal thiolase (Figure 5B). The matrix of peroxisomes was distinctly stained, whereas no label was detected in the cytosol. Treatment with clofibrate led to an enhanced labelling of thiolase in peroxisomes (Figure 5C). Importantly, clofibrate-dependent proliferation of peroxisomes resulted in a clear detection of L-FABP in the peroxisomal matrix although the labelling was lower than that in the cytosol (Figures 5D and 5E). Interestingly, some proliferated peroxisomes also exhibited an intense crown-like labelling of the outer surface of the membrane (see Figure 5D). In Figure 5(E), the nucleoids (marked as Nu) are clearly visible, indicating that the picture shown represents a true cut through the centre of a peroxisome and not just a peripheral cut at the top of a particle. In contrast with peroxisomes, the presence of the gold particles in mitochondria was barely detectable (Figure 5F). The apparent absence of the labelling of L-FABP in normal peroxisomes, which has been mentioned in previous reports [11,12] and confirmed by our study, may be attributed to the low content of this protein in normal peroxisomes, which is beyond the detection ability of the immunogold technique.

Subcellular localization of the GFP–FABP fusion protein

The broad consensus sequence of PTS1 (S/A/C/K/N-K/R/H/Q/N-L/I) [36,37] implies possible differences in the efficiency of interaction of the PTS1-containing proteins with the corresponding receptor Pex5p that may result in only partial import of some proteins into peroxisomes. Indeed, previous studies strongly support this suggestion [38,39]. The extreme C-terminus of L-FABP (KRI_{COOH}) is in accordance with the PTS1 consensus sequence, implying possible interaction of L-FABP with Pex5p, although this interaction might be weak. Noteworthily, the C-terminus of L-FABP is strictly conserved within L-FABPs from different mammals. In contrast, within the whole family of FABPs, only the C-terminus of L-FABP shows similarity to the PTS1 consensus sequence (results not shown). To test whether or not the KRI_{COOH} sequence in rat L-FABP represents a targeting signal for peroxisomes, we constructed vectors expressing L-FABP as a fusion protein behind GFP (see the Materials and methods section). CHO cells were transfected with the constructs and analysed by fluorescence microscopy. Under both conditions, only a diffuse cytosolic staining pattern was observed (results not shown). Permeabilization of the transfected cells with digitonin, which results in the leakage of cytosol from the cells, did not reveal the appearance of any punctate pattern characteristic for peroxisomes or other subcellular organelles. We also expressed N-terminally His-tagged L-FABP in *E. coli* and analysed the interaction of the recombinant protein with a biotinylated human Pex5p fusion protein [31]. Under the conditions used, the expressed L-FABP was not recognized by Pex5p (results not shown).

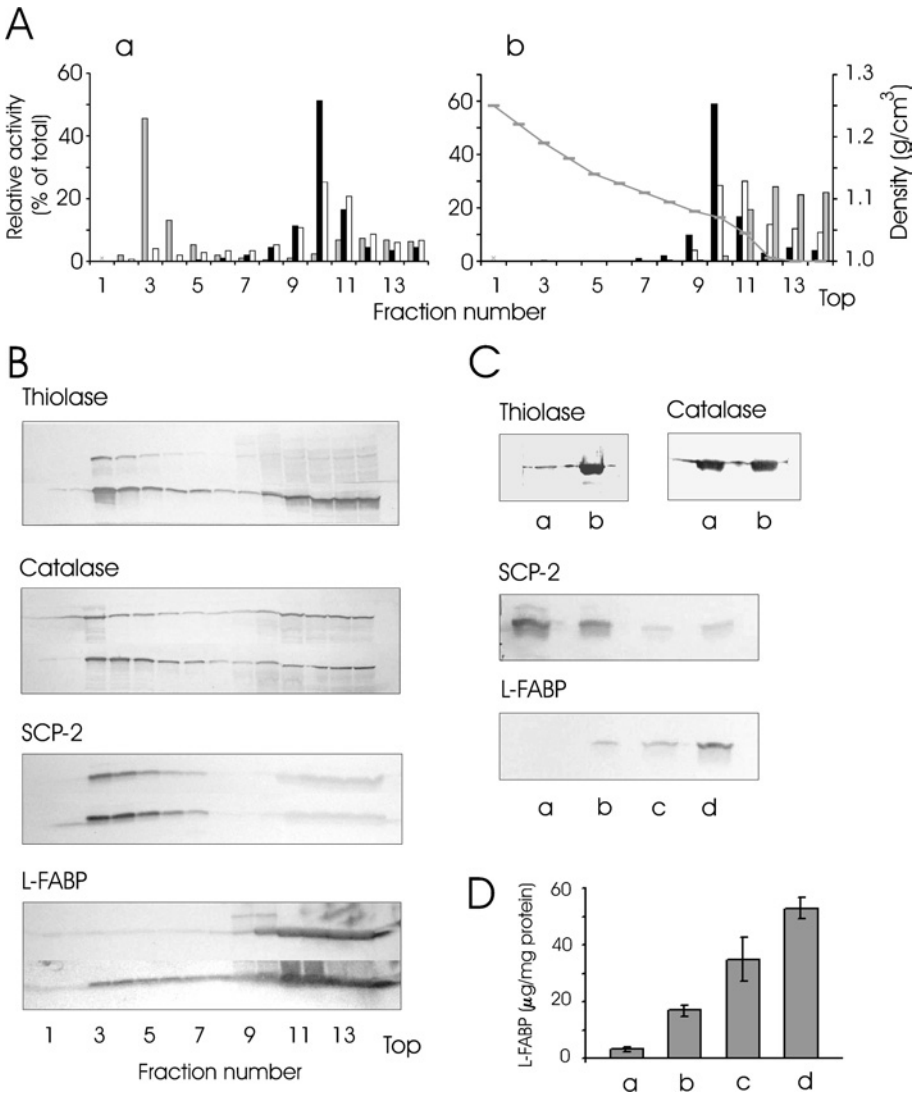

Figure 3 Effect of clofibrate treatment on the subcellular distribution of L-FABP

(**A**) Optiprep gradient centrifugation of a post-nuclear supernatant prepared from clofibrate-treated rat livers. Fractions were analysed for protein content (**a**, open bars) and marker enzyme activities: L-α-hydroxyacid dehydrogenase (**a**, grey bars), glutamate dehydrogenase (**a**, filled bars), esterase (**b**, open bars), glucose-phosphate isomerase (**b**, grey bars) and acid phosphatase (**b**, filled bars). The ordinate axis (left) represents the relative enzyme activities in each fraction (percentage of the total activity loaded on the gradient). The recoveries of the enzyme activities and protein content were between 89 and 115 %. (**B**) Proteins derived from equal volumes of each fraction (see **A**) were separated by SDS/PAGE and immunoblotted (upper bands, normal rat liver; lower bands, clofibrate-treated rat liver). (**C**, **D**) Quantitative estimation of proteins in normal (a) or proliferated (b) peroxisomes and in cytosol isolated from normal (c) or clofibrate-treated (d) rat liver. The proteins were detected by immunoblotting (**C**) or by ELISA (**D**). Samples with equal amounts of protein content were used. For immunoblotting, the aliquots of fractions 3 and 13 from the Optiprep gradients (see **A**) were used. The immunosignal reflecting the position of L-FABP on the line 'a' was only barely detectable. The peroxisomes used for the ELISA were isolated by employing the standard procedure (see the Materials and methods section). The cytosol was prepared by differential centrifugation. Values are means $\pm$ S.D. ($n = 3$).

Possible role of L-FABP as a facilitator of peroxisomal enzymatic activities

We studied the effect of native L-FABP isolated from rat liver cytosol on the activity of palmitoyl-CoA β-oxidation in peroxisomes (Figure 6A) and the thioesterase activity towards acyl-CoAs with different chain lengths (Figure 6B). In the absence of lipid-binding proteins, the substrate curve for β-oxidation of palmitoyl-CoA revealed a strong inhibition at elevated substrate concentrations (Figure 6A, curve 1). As expected from the results obtained previously for separate peroxisomal β-oxidation enzymes [34], this inhibition was abolished by the addition of albumin (Figure 6A, curve 2). Likewise, the addition of L-FABP led to a strong activation of peroxisomal β-oxidation (Figure 6A, curve 3). The stimulatory effect was especially evident at palmitoyl-CoA concentrations in the range 10–20 μM. This probably reflects the 1:2 stoichiometry of the L-FABP (8 μM) interaction with long-chain acyl-CoAs.

Addition of purified L-FABP to peroxisomal matrix proteins stimulated the total thioesterase activity with medium-chain and especially with long-chain acyl-CoAs but had no effect on the activity with short-chain acyl-CoAs (Figure 6B, right panel).

Ability of soluble peroxisomal proteins to bind long-chain fatty acids and the effect of clofibrate

Size-exclusion chromatography led to an effective separation of low molecular mass proteins including L-FABP and SCP-2 from the bulk of peroxisomal matrix proteins (Figure 7A, fraction II).

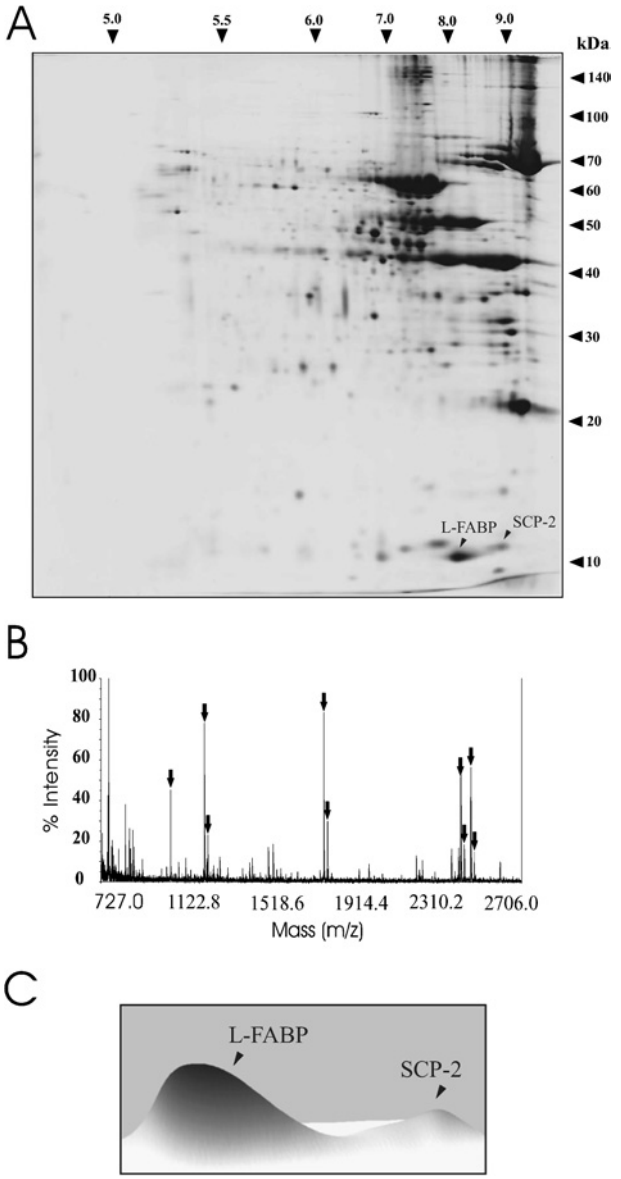

Figure 4 Two-dimensional gel electrophoresis of peroxisomal matrix proteins and detection of L-FABP

(**A**) Two-dimensional gel of matrix proteins (300 μg) extracted from clofibrate-treated rat liver peroxisomes. Apparent pI and molecular mass values are indicated. Localization of L-FABP and SCP-2 in the gel is marked by arrowheads. (**B**) Mass spectrum of the peptide fingerprint obtained after trypsin digestion of the excised spot marked on the gel as L-FABP (see **A**). The arrows indicate the peptides that match within 20 p.p.m. to the predicted peptides of L-FABP. (**C**) Comparison of the spot intensities of L-FABP and SCP-2.

Soluble matrix proteins from normal rat liver peroxisomes showed a relatively low capacity to bind oleic acid (Figure 7A, left panel). Treatment with clofibrate led to a marked increase in the oleic acid binding capacity of peroxisomal matrix proteins (Figure 7A, right panel). Importantly, nearly all radioactivity bound to peroxisomal proteins (about one-quarter of the total radioactivity loaded on to the column) was recovered in fraction II containing L-FABP and SCP-2. Western-blot analysis confirmed that this fraction contained a lower amount of SCP-2 as compared with normal peroxisomes, while the content of L-FABP was drastically increased (Figure 7B, left panels compared with right panels).

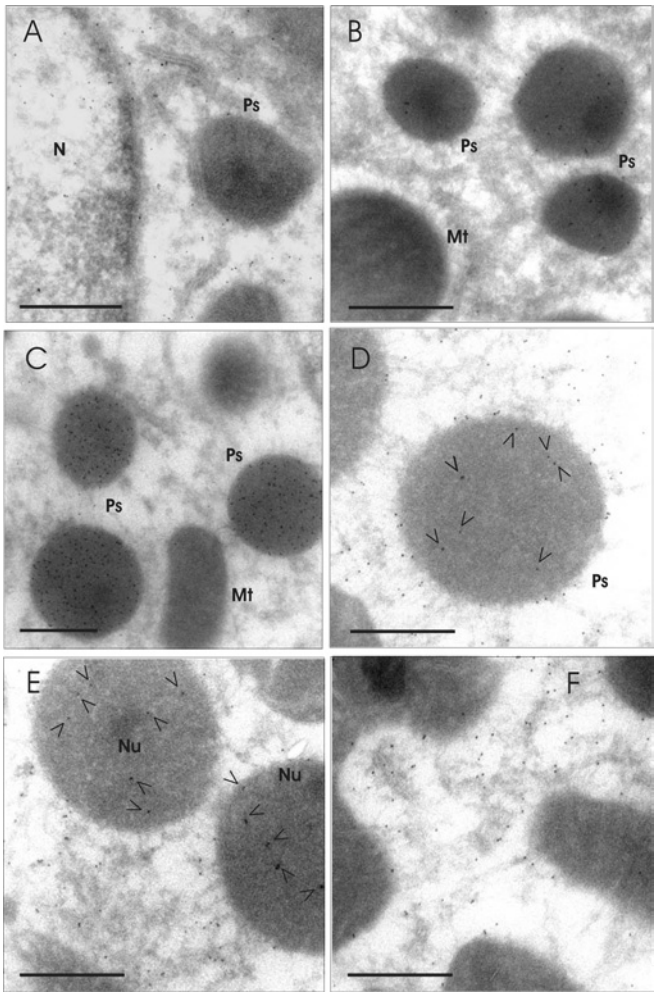

Figure 5 Immunogold detection of L-FABP

The liver sections were incubated with antibodies against L-FABP (**A**, **D**–**F**) or thiolase (**B**, **C**) followed by Protein A–gold. Sections of normal (**A**, **B**) or clofibrate-treated (**C**–**F**) rat livers are shown. The arrowheads in (**D**, **E**) indicate positions of the gold particles in peroxisomes. Ps, peroxisomes; Mt, mitochondria; N, nucleus; Nu, nucleoids. Original magnification, $\times$15000 (**A**, **B**, **D**–**F**) or $\times$11000 (**C**); scale bar, 500 nm. Control preparations (incubation without antibodies) did not contain immunogold labels (results not shown).

Further study of the capacity of column fraction II to bind NEFAs was performed under equilibrium conditions by using the fluorescent ligand *cis*-parinaric acid. The results indicated a significant level of the *cis*-parinaric acid binding capacity in the fraction II from clofibrate-treated rats (Figure 8). In contrast, control fraction II showed a markedly lower *cis*-parinaric acid binding capacity. Mathematical analysis revealed the presence of a binding site with high affinity for *cis*-parinaric acid ($K_d = 0.13 \pm 0.04$ μM) when samples from clofibrate-treated rats were used. The same assay of control samples showed the presence of a binding site with much lower affinity ($K_d = 0.38 \pm 0.07$ μM).

DISCUSSION

Three largely independent approaches were employed to investigate the subcellular distribution of L-FABP in rat liver: (i) analytical subcellular fractionation with immunodetection of L-FABP in isolated organellar fractions; (ii) two-dimensional gel electrophoresis of peroxisomal matrix proteins followed by MS

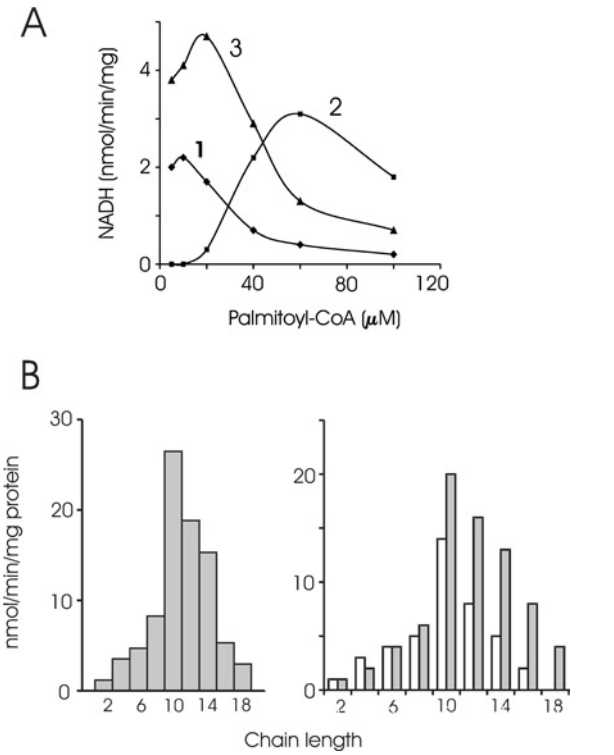

Figure 6 Effect of L-FABP on the enzymatic activities in purified peroxisomes

(**A**) Dependence of peroxisomal β-oxidation on palmitoyl-CoA concentration. Curve 1, control without any additions; curve 2, 9 μM BSA; curve 3, 8 μM L-FABP. The fraction of delipidated matrix proteins isolated from normal rat liver peroxisomes was used. (**B**) Acyl-CoA thioesterase substrate specificity in the whole peroxisomal fraction (left panel) and in the fraction of peroxisomal matrix proteins (right panel). The activity in the whole peroxisomal fraction was measured in the presence of 3 μM BSA (0.02%). Activity measurements in the peroxisomal matrix fraction were performed without any additions (open bars) or in the presence of 8 μM L-FABP (grey bars). Concentration of acyl-CoA esters was 20 μM. Peroxisomes were isolated from clofibrate-treated rat liver.

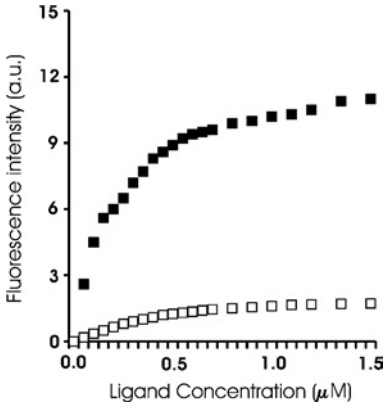

Figure 8 Clofibrate treatment significantly increases the *cis*-parinaric acid binding ability of the peroxisomal matrix proteins

Aliquots (1 mg of protein/0.5 ml) of delipidated matrix protein fractions obtained from control or clofibrate-treated rat liver peroxisomes were fractionated on Superdex G-75 (without oleic acid, see Figure 7). Fractions 20–23 containing low molecular mass proteins were combined and concentrated by using membrane filters with a cutoff of 5 kDa. The resulting samples were of equal volume but contained different amounts of total protein. Aliquots of these samples containing 4 μg of protein (control; □) or 6 μg of protein (clofibrate; ■) were titrated with increasing amounts of *cis*-parinaric acid. Emission was monitored using a fluorescence spectrophotometer ($\lambda_{ex} = 310$ nm and $\lambda_{em} = 416$ nm). The binding experiments were performed at least three times. The results of one representative experiment are shown.

analysis and (iii) immunoelectron microscopy applied to liver sections. The results clearly demonstrate that L-FABP is indeed present in the matrix of rat liver peroxisomes. In addition, the results show a strong induction of peroxisomal L-FABP after treatment of rats with clofibrate. Under these conditions, peroxisomal L-FABP content increased more than the total cellular L-FABP content, suggesting a more efficient translocation into peroxisomes after drug treatment. However, the *in vivo* targeting experiments using GFP–FABP fusion proteins and analysis of the binding of recombinant L-FABP to Pex5p *in vitro* were unable to demonstrate an involvement of the PTS1-dependent pathway in

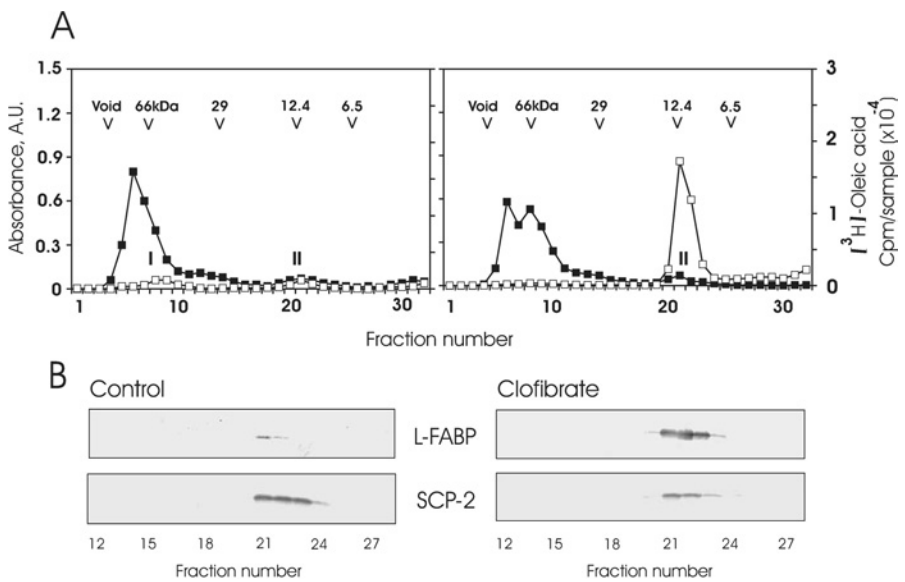

Figure 7 Effect of clofibrate treatment on the oleic acid binding capacity of peroxisomal matrix proteins

Soluble matrix proteins (1 mg) isolated from normal (**A**, **B**, left panels) or clofibrate-treated (**A**, **B**, right panels) rat liver peroxisomes were incubated with [^{3}H]oleic acid and subjected to Superdex 75 gel chromatography. (**A**) Fractions (0.5 ml) were analysed for absorbance at 280 nm (■) and radioactivity (□). A.U., absorbance units. The positions of the molecular mass marker proteins are indicated by arrowheads. (**B**) Proteins from each fraction were separated by SDS/PAGE, blotted and immunostained with antibodies against L-FABP and SCP-2.

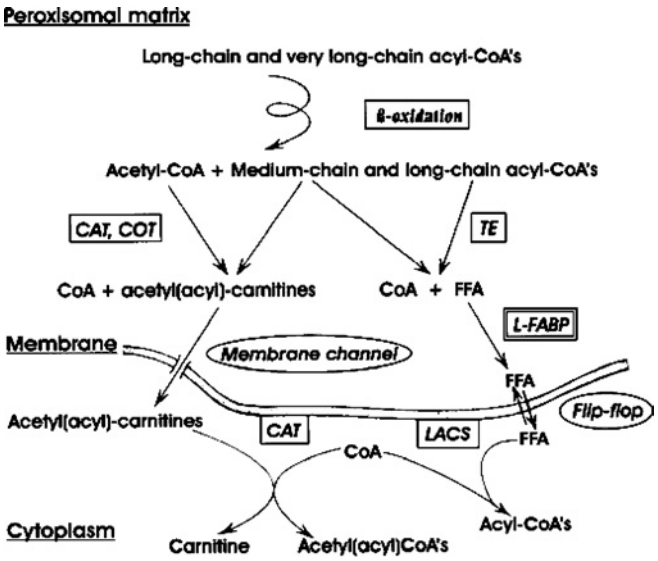

Figure 9 Putative function of L-FABP in the export of medium- and long-chain fatty acids out of peroxisomes

Abbreviations: CAT, carnitine acetyltransferase; COT, carnitine octanoyltransferase; TE, acyl-CoA thioesterase; FFA, NEFA. According to our recent observations [35], mammalian peroxisomal membrane channels allow free transmembrane movement of small solutes, e.g. urate and glycolate, but heavily restrict permeation of larger molecules such as cofactors (CoA, NAD/H and NADP/H). Therefore the intraperoxisomal acetyl(acyl)-CoA esters must be transformed into compounds capable of penetrating the peroxisomal membrane [e.g. acetyl(acyl)-carnitines or NEFAs]. Note that a significant part of peroxisomal CAT activity is membrane-bound (V. D. Antonenkov, unpublished work), implying a possible role of the enzyme in 'vectorial acetylation' that would then serve as the driving force for the export of acetyl moieties out of the peroxisomes. A similar role may be attributed to LACS4, the enzyme responsible for 'vectorial acylation' of long-chain fatty acids. Binding of non-esterified fatty acids to peroxisomal L-FABP may accelerate their transport inside the particles and facilitate their insertion into the membrane.

the targeting of L-FABP to peroxisomes. These negative findings suggest two possibilities: (i) the poor interaction of L-FABP with Pex5p results in PTS1-dependent translocation rates that are below the detection limits of our assays, or (ii) L-FABP may be targeted to peroxisomes via mechanisms that are independent of its own putative PTS1 (e.g. a 'piggy-back' mechanism) [36].

The presence of L-FABP side by side with SCP-2 in rodent liver peroxisomes makes a revision of the possible functions of these proteins necessary. Recent studies on knockout mouse models have revealed a participation of L-FABP and SCP-2 in the metabolism of lipid-soluble compounds such as long straight-chain and branched-chain fatty acids [19–23,40]. Our present results point towards a role of L-FABP in facilitating palmitoyl-CoA β-oxidation by peroxisomal enzymes, a function that was previously attributed to SCP-2 [40]. The clofibrate-dependent induction of L-FABP without a concomitant increase in SCP-2 in proliferated peroxisomes implies the existence of a specific function for each of these proteins. The induction of L-FABP goes hand in hand with the induction of the peroxisomal β-oxidation pathway for long- and very-long-straight-chain fatty acids. Importantly, peroxisomal β-oxidation does not proceed to completion and as a result generates long-and medium-chain acyl-CoAs along with acetyl-CoA (reviewed in [3,41]). As depicted in Figure 9, acetyl-CoA and medium-chain acyl-CoAs may be converted into the corresponding carnitine derivatives inside peroxisomes by carnitine acetyl- and octanoyl-transferases (reviewed in [42]). Both enzymes are inducible by clofibrate. Acetyl(acyl)carnitines, owing to their size that is much smaller than the size of acetyl-(acyl)-CoA derivatives, are able to cross the peroxisomal membrane through the pore-forming channels recently described by us [43]. In contrast, the absence from peroxisomes of carnitine palmitoyltransferase prevents the formation of long-chain acyl-carnitines. Instead, a set of clofibrate-inducible peroxisomal acyl-CoA thioesterases (reviewed in [44]) cleaves off acyl-CoAs into CoA and NEFAs. The latter may directly diffuse through the membrane by means of a flip-flop mechanism (reviewed in [45]). The clofibrate-dependent increase in the capacity of peroxisomal matrix proteins to bind oleic acid and *cis*-parinaric acid, as shown here, is in accordance with the induction of L-FABP but does not correlate with the stable level of SCP-2 in peroxisomes. This suggests that L-FABP may play a role in binding and, hence, solubilizing the enlarged (owing to induction of thioesterases), pool of NEFAs in the proliferated peroxisomes. Moreover, L-FABP is able to transfer NEFAs directly to membranes [46]. On the other hand, the relatively low content of thioesterases and L-FABP in normal peroxisomes may lead to a more complete oxidative degradation of acyl-CoAs, resulting in generation of medium-chain derivatives capable of interacting with carnitine octanoyltransferase. Interestingly, the flip-flop mechanism predicts an unexpected role for LACS4 (long-chain acyl-CoA synthetase 4), which is located at the outer surface of peroxisomal membranes [47]. This enzyme may participate in a process termed 'vectorial acylation' (reviewed in [48]) facilitating the diffusion of NEFAs out of peroxisomes (see Figure 9) rather than being involved, as is currently believed, in the synthesis of acyl-CoAs for their import into the particles [47]. Our suggestion may help to clarify the confusion about the metabolic role of LACS4 as related to triacylglycerol synthesis [49]. The long-chain fatty acids exported from peroxisomes and activated by LACS4 might be used for the synthesis of triacylglycerols, thereby providing a direct link between peroxisomal β-oxidation of very-long-chain fatty acids and formation of storage lipids.

This work was supported by the Academy of Finland, Sigrid Juselius Foundation and European Union (contract no. PL51208).

REFERENCES

1 Zimmerman, A. W. and Veerkamp, J. H. (2002) New insights into the structure and function of fatty acid-binding proteins. Cell. Mol. Life Sci. **59**, 1096–1116
2 Haunerland, N. H. and Spener, F. (2004) Fatty acid-binding proteins – insights from genetic manipulations. Prog. Lipid Res. **43**, 328–349
3 Reddy, J. K. (2004) Peroxisome proliferators and peroxisome proliferators-activated receptor α. Am. J. Pathol. **164**, 2305–2321
4 Kaikaus, R. M., Chan, W. K., Ortiz de Montellano, P. R. and Bass, N. M. (1993) Mechanism of regulation of liver fatty acid-binding protein. Mol. Cell. Biochem. **123**, 93–100
5 Wolfrum, C., Ellinghaus, P., Fobker, M., Seedorf, U., Assmann, G., Börchers, T. and Spener, F. (1999) Phytanic acid is ligand and transcriptional activator of murine liver fatty acid binding protein. J. Lipid Res. **40**, 708–714
6 Wolfrum, C., Borrmann, C. M., Börchers, T. and Spener, F. (2001) Fatty acids and hypolipidemic drugs regulate peroxisome proliferators-activated receptors α- and γ-mediated gene expression via liver fatty acid binding protein: a signaling path to the nucleus. Proc. Natl. Acad. Sci. U.S.A. **98**, 2323–2328
7 Capron, F., Coltoff-Schiller, B., Johnson, A. B., Fleischner, G. M. and Goldfischer, S. (1979) Immunocytochemical localization of hepatic ligandin and Z protein utilizing frozen sections for light and electron microscopy. J. Histochem. Cytochem. **27**, 961–966
8 Appelkvist, E. L. and Dallner, G. (1980) Possible involvement of fatty acid binding protein in peroxisomal β-oxidation of fatty acids. Biochim. Biophys. Acta **617**, 156–160
9 Iseki, S., Kondo, H., Hitomi, M. and Ono, T. (1988) Immunocytochemical localization of hepatic fatty acid binding protein in the liver of fed and fasted rats. Histochemistry **89**, 317–322
10 Paulussen, R. J., Geelen, M. J., Beynen, A. C. and Veerkamp, J. H. (1989) Immunochemical quantitation of fatty-acid-binding proteins. I. Tissue and intracellular distribution, postnatal development and influence of physiological conditions on rat heart and liver FABP. Biochim. Biophys. Acta **1001**, 201–209

11 Bordewick, U., Heese, M., Börchers, T., Robenek, H. and Spener, F. (1989) Compartmentation of hepatic fatty-acid-binding protein in liver cells and its effect on microsomal phosphatidic acid biosynthesis. Biol. Chem. Hoppe-Seyler **370**, 229–238

12 Fahimi, H. D., Voelkl, A., Vincent, S. H. and Muller-Eberhard, U. (1990) Localization of the heme-binding protein in the cytoplasm and of a heme-binding protein-like immunoreactive protein in the nucleus of rat liver parenchymal cells. Hepatology **11**, 859–865

13 Chao, H., Zhou, M., McIntosh, A., Schroeder, F. and Kier, A. B. (2003) ACBP and cholesterol differently alter fatty acyl CoA utilization by microsomal ACAT. J. Lipid Res. **44**, 72–83

14 Jefferson, J. R., Slotte, J. P., Nemecz, G., Pastuszyn, A., Scallen, T. J. and Schroeder, F. (1991) Intracellular sterol distribution in transfected mouse L-cell fibroblasts expressing rat liver fatty acid-binding protein. J. Biol. Chem. **266**, 5486–5496

15 Jolly, C. A., Wilton, D. C. and Schroeder, F. (2000) Microsomal fatty acyl-CoA transacylation and hydrolysis: fatty acyl-CoA species dependent modulation by liver fatty acyl-CoA binding proteins. Biochim. Biophys. Acta **1483**, 185–197

16 Reubsaet, F. A., Veerkamp, J. H., Bruckwilder, M. L., Trijbels, J. M. and Monnens, L. A. (1990) The involvement of fatty acid binding protein in peroxisomal fatty acid oxidation. FEBS Lett. **267**, 229–230

17 Seedorf, U., Ellinghaus, P. and Nofer, J. R. (2000) Sterol carrier protein-2. Biochim. Biophys. Acta **1486**, 45–54

18 Murphy, E. J., Prows, D. R., Jefferson, J. R. and Schroeder, F. (1996) Liver fatty acid binding protein expression in transfected fibroblasts stimulates fatty acid uptake and metabolism. Biochim. Biophys. Acta **1301**, 191–198

19 Newberry, E. P., Xie, Y., Kennedy, S., Han, X., Buhman, K. K., Luo, J., Gross, R. W. and Davidson, N. O. (2003) Decreased hepatic triglyceride accumulation and altered fatty acid uptake in mice with deletion of the liver fatty acid-binding protein gene. J. Biol. Chem. **278**, 51664–51672

20 Martin, G. G., Danneberg, H., Kumar, L. S., Atshaves, B. P., Erol, E., Bader, M., Schroeder, F. and Binas, B. (2003) Decreased liver fatty acid binding capacity and altered liver lipid distribution in mice lacking the liver fatty acid-binding protein gene. J. Biol. Chem. **278**, 21429–21438

21 Erol, E., Kumar, L. S., Cline, G. W., Shulman, G. I., Kelly, D. P. and Binas, B. (2004) Liver fatty acid-binding protein is required for high rates of hepatic fatty acid oxidation but not for the action of PPAR-α in fasting mice. FASEB J. **18**, 347–349

22 Atshaves, B. P., McIntosh, A. L., Payne, H. R., Mackie, J., Kier, A. B. and Schroeder, F. (2005) Effect of branched-chain fatty acid on lipid dynamics in mice lacking liver fatty acid binding protein gene. Am. J. Physiol. Cell Physiol. **288**, C543–C558

23 Atshaves, B. P., McIntosh, A. M., Lyukyutova, O. I., Zipfel, W., Webb, W. W. and Schroeder, F. (2004) Liver fatty acid-binding protein gene ablation inhibits branched-chain fatty acid metabolism in cultured primary hepatocytes. J. Biol. Chem. **279**, 30954–30965

24 Atshaves, B. P., Storey, S. M., Huang, H. and Schroeder, F. (2004) Liver fatty acid binding protein expression enhances branched-chain fatty acid metabolism. Mol. Cell. Biochem. **259**, 115–129

25 Antonenkov, V. D., Sormunen, R. T. and Hiltunen, J. K. (2004) The behavior of peroxisomes *in vitro*: mammalian peroxisomes are osmotically sensitive particles. Am. J. Physiol. Cell Physiol. **287**, C1623–C1635

26 Fujiki, Y., Fowler, S., Shio, H., Hubbard, A. L. and Lazarow, P. B. (1982) Polypeptide and phospholipids composition of the membrane of rat liver peroxisomes. Comparison with endoplasmic reticulum and mitochondrial membranes. J. Cell Biol. **93**, 103–110

27 Antonenkov, V. D. (1989) Dehydrogenases of the pentose phosphate pathway in rat liver peroxisomes. Eur. J. Biochem. **183**, 75–82

28 Murphy, E. J., Edmondson, R. D., Russel, D. H., Colles, S. and Schroeder, F. (1999) Isolation and characterization of two distinct forms of liver fatty acid binding protein from the rat. Biochim. Biophys. Acta **1436**, 413–425

29 Ohlmeier, S., Kastaniotis, A., Hiltunen, J. K. and Bergmann, U. (2004) The yeast mitochondrial proteome, a study of fermentative and respiratory growth. J. Biol. Chem. **279**, 3956–3979

30 Fransen, M., Wylin, T., Brees, C., Mannaerts, G. P. and Van Veldhoven, P. P. (2001) Human Pex19p binds peroxisomal integral membrane proteins at regions distinct from their sorting sequences. Mol. Cell. Biol. **21**, 4413–4424

31 Fransen, M., Terlecky, S. R. and Subramani, S. (1998) Identification of a human PTS1 receptor docking protein directly required for peroxisomal protein import. Proc. Natl. Acad. Sci. U.S.A. **95**, 8087–8092

32 Slot, J. W. and Geuze, H. J. (1985) A new method of preparing gold probes for multiple-labeling cytochemistry. Eur. J. Cell Biol. **38**, 87–93

33 Frolov, A., Cho, T.-H., Murphy, E. J. and Schroeder, F. (1997) Isoforms of rat liver fatty acid binding protein differ in structure and affinity for fatty acids and fatty acyl CoAs. Biochemistry **36**, 6545–6555

34 Antonenkov, V. D., Van Veldhoven, P. P., Waelkens, E. and Mannaerts, G. P. (1997) Substrate specificities of 3-oxoacyl-CoA thiolase A and sterol carrier protein 2/3-oxoacyl-CoA thiolase purified from normal rat liver peroxisomes. J. Biol. Chem. **272**, 26023–26031

35 Antonenkov, V. D., Sormunen, R. T. and Hiltunen, J. K. (2004) The rat liver peroxisomal membrane forms a permeability barrier for cofactors but not for small metabolites *in vitro*. J. Cell Sci. **117**, 5633–5642

36 Subramany, S., Koller, A. and Snyder, W. B. (2000) Import of peroxisomal matrix and membrane proteins. Annu. Rev. Biochem. **69**, 399–418

37 Amery, L., Fransen, M., De Nys, K., Mannaerts, G. P. and Van Veldhoven, P. P. (2000) Mitochondrial and peroxisomal targeting of 2-methylacyl-CoA racemase in humans. J. Lipid Res. **41**, 1752–1759

38 Lametschwandtner, G., Brocard, C., Fransen, M., Van Veldhoven, P., Berger, J. and Hartig, A. (1998) The difference in recognition of terminal tripeptides as peroxisomal targeting signal 1 between yeast and human is due to different affinities of their receptor Pex5p to the cognate signal and to residues adjacent to it. J. Biol. Chem. **273**, 33635–33643

39 Legakis, J. L., Koepke, J. I., Jedeszko, C., Barlaskar, F., Terlecky, L. J., Edwards, H. J., Walton, P. A. and Terlacky, S. R. (2002) Peroxisome senescence in human fibroblasts. Mol. Biol. Cell **13**, 4243–4255

40 Seedorf, U., Raabe, M., Ellinghaus, P., Kannenberg, F., Fobker, M., Engel, T., Denis, S., Wouters, F., Wirtz, K. W. A., Wanders, R. et al. (1998) Defective peroxisomal catabolism of branched fatty acyl coenzyme A in mice lacking the sterol carrier protein-2/sterol carrier protein-x gene function. Genes Dev. **12**, 1189–1201

41 Hiltunen, K. J., Mursula, A. M., Rottensteiner, H., Wierenga, R. K., Kastaniotis, A. J. and Gurvitz, A. (2003) The biochemistry of peroxisomal β-oxidation in the yeast *Saccharomyces cerevisiae*. FEMS Microbiol. Rev. **27**, 34–64

42 Ramsay, R. R. (1999) The role of the carnitine system in peroxisomal fatty acid oxidation. Am. J. Med. Sci. **318**, 28–35

43 Antonenkov, V. D., Rokka, A., Sormunen, R. T., Benz, R. and Hiltunen, J. K. (2005) Solute traffic across mammalian peroxisomal membrane – single channel conductance monitoring reveals pore-forming activities in peroxisomes. Cell. Mol. Life Sci. **62**, 2886–2895

44 Hunt, M. C. and Alexson, S. E. H. (2002) The role acyl-CoA thioesterases play in mediating intracellular lipid metabolism. Prog. Lipid Res. **41**, 99–130

45 Hamilton, J. A. (2003) Fast flip-flop of cholesterol and fatty acids in membranes: implications for membrane transport proteins. Curr. Opin. Lipidol. **14**, 263–271

46 Corsico, B., Liou, H. L. and Storch, J. (2004) The α-helical domain of liver fatty acid binding protein is responsible for the diffusion-mediated transfer of fatty acids to phospholipid membranes. Biochemistry **43**, 3600–3607

47 Lewin, T. M., Van Horn, C. G., Krisans, S. K. and Coleman, R. A. (2002) Rat liver acyl-CoA synthetase 4 is a peripheral-membrane protein located in two distinct subcellular organelles, peroxisomes and mitochondrial-associated membrane. Arch. Biochem. Biophys. **404**, 263–265

48 Black, P. N. and DiRusso, C. C. (2003) Transmembrane movement of exogenous long-chain fatty acids: proteins, enzymes, and vectorial esterification. Microbiol. Mol. Biol. Rev. **67**, 454–472

49 Lewin, T. M., Kim, J.-H., Granger, D. A., Vance, J. E. and Coleman, R. A. (2001) Acyl-CoA synthetase isoforms 1, 4, and 5 are present in different subcellular membranes in rat liver and can be inhibited independently. J. Biol. Chem. **276**, 24674–24679

Received 30 June 2005/31 October 2005; accepted 1 November 2005
Published as BJ Immediate Publication 1 November 2005, doi:10.1042/BJ20051058